

DESY-Bibliothek

21. NOV. 1967

~~Herrn Dr. Mellentin~~

R 3

DEUTSCHES ELEKTRONEN-SYNCHROTRON **DESY**

DESY 67/31

October 1967

ELECTROPRODUCTION OF PIONS

by

H. Blechschmidt, J.P. Dowd, B. Elsner, K. Heinloth

P. Karow, J. Rathje, D. Schmidt, J.H. Smith

Deutsches Elektronen-Synchrotron DESY, Hamburg, Germany

and

A. Kanaris, A.G. Wynroe

University of Manchester, England

2 HAMBURG 52 . NOTKESTIEG 1

ELECTROPRODUCTION OF PIONS

by

H. Blechschmidt, J.P. Dowd*, B. Elsner, K. Heinloth,
P. Karow, J. Rathje, D. Schmidt, J.H. Smith**,+

Deutsches Elektronen-Synchrotron DESY, Hamburg, Germany

and

A. Kanaris, A.G. Wynroe

University of Manchester, England

* Present address: SMTI, New Bedford, Massachusetts, U. S. A.

** Present address: University of Illinois, Urbana, Illinois, U. S. A.

+ supported by Volkswagen foundation

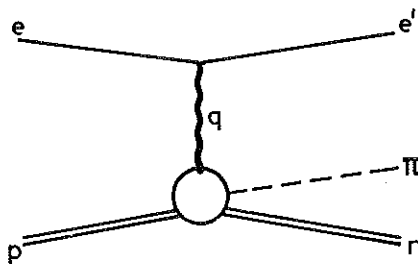
During the last years, electroproduction of positive pions was studied (1,2) performed at energies in the region of the first nucleon resonance in coincidence experiments by several groups. We report a spark chamber experiment done at energies of the virtual photon from 0.7 GeV up to 3 GeV as improved with respect to an earlier version (3). We measured electroproduction of single positive pions on hydrogen, detecting the scattered electron and the produced pion in coincidence:

$$(1) \quad e + p \rightarrow e' + \pi^+ + n$$

In addition to particles from this reaction, we also detected positive or negative pions from multiple-pion production:

$$(2) \quad e + p \rightarrow e' + \pi^\pm + (N + \pi + \dots)$$

The single-pion production process is described by the following diagram:



The four-momenta are written as e for the incoming electron, e' for the scattered electron, q for the virtual photon, π^+ for the produced pion, p for the target proton and n for the recoiling neutron.

Production angles and the momenta of the scattered electron and of the produced pion were measured in a detection apparatus consisting of two pairs of spark chambers and the deflection magnet MH. Pions and electrons were identified by a threshold Čerenkov counter Č and two thick-plate spark chambers SC5 and SC6. Pictures were photographed whenever two charged particles passed the spark chamber system. The intensity of the primary electron beam was monitored by an ionisation chamber IC which was calibrated against a quantameter. The beam was absorbed inside the magnet MH by a tungsten beam catcher A.

To separate single-pion production (1) from reaction (2), we calculated the mass m_X of the unobserved particle system. In the case of single positive pion production, the mass m_X must be equal to the mass of the

recoiling neutron, whereas in multiple-pion production the missing mass m_X is greater than the nucleon mass by at least one pion mass. In reactions where a negative pion was detected, this pion could only arise from multiple-pion production. In Fig. 2 we plotted the spectra of the missing mass m_X for both positive and negative pion production in three intervals of the virtual photon energy q_0 .

In Fig. 2a the mass of the recoiling nucleon shows up clearly. One can see that the single-pion production is the dominating process in this energy region. Multiple-pion production dominates at higher energies of the virtual photon, as can be seen in Figs. 2b and 2c. The events with masses around the neutron mass were fitted with a Gaussian distribution with a half-width of ± 80 MeV (solid curves). All the events in Figs. 2b and 2c lying in the region $0.8 < m_X < 1.05$ GeV were treated as events of single-pion production. In calculating the cross section, the $\pm 10\%$ error due to possible overlapping of single-pion peak and multiple-pion distribution was taken into account.

For gathering information about the multiple-pion production process, we did a Monte-Carlo calculation for the mass distribution m_X , assuming ρ^0 electroproduction in the limit of small q^2 . The well known diffraction behavior in the photoproduction of ρ^0 mesons was taken into account. The dashed curves in Figs. 2b and 2c are the results of this calculation; they have been normalized to the experimental data. It can be seen that the main contribution to multiple-pion production is due to ρ^0 production.

Figures 3a-c show the distribution of the squared four-momentum of the virtual photon for the single-pion production events in the three energy intervals. The acceptance ACC was calculated by integration over the accepted region of azimuthal angles of the electron and the pion. The virtual photons in the observed processes are close to the mass shell. The main contribution arises at $|q^2| \lesssim 0.1$ GeV².

The cross section $\frac{d\sigma}{dt}$ for electroproduction as a function of the four-momentum transfer t to the nucleon is shown in Figs. 4a-c. We got these values by integrating over the accepted region of q^2 and averaging over the interval of the squared total energy in the pion-nucleon system $s' = (q + p)^2$ and over the azimuthal angle ϕ subtended by the plane defined by the virtual photon and the pion and the plane defined by

the incoming and outgoing electron. The ϕ distribution of all measured events is compatible with isotropy, as can be seen in Figs. 5a-c. The results were corrected for absorption of pions inside the target as well as for pion decay, for bremsstrahlung of incoming and outgoing electrons, and for errors in particle identification. In all figures and calculations we have neglected those few events where the acceptance was less than 1% of the mean value.

In the limit $q^2 \rightarrow 0$, where q^2 is the mass of the virtual photon, the connection between the electroproduction of pions and the photoproduction of pions by unpolarized photons is given^(4,5) by

$$(3) \left(\frac{d^3\sigma}{ds' dq^2 dt} \right)_{\text{electro-production}} = \frac{\alpha (s' - M_p^2)}{2\pi (s - M_p^2)^2 |q^2|} \left[1 + \frac{2(s - M_p^2)(s - s')}{(s' - M_p^2)^2} \right] \left(\frac{d\sigma}{dt} \right)_{\text{photo-production}}$$

For the purpose of ascertaining whether our data lay in this small q^2 limit we compared the q^2 distributions in Figs. 3a-c with the predicted $1/q^2$ behavior (see Equ.(3)) as indicated by the dashdotted curves. The rather fair fit permits us to apply Equ. (3) to our data. By means of this formula, we compare experimental results from photoproduction of positive pions^(6,7) with our measured cross sections. We find good agreement, as can be seen in Figs. 4a-c.

Acknowledgements

We wish to thank Professors W. Jentschke and P. Stähelin for their continued interest and encouragement during this experiment. Two of us (A.K. and A.G.W.) thank Professor P. Murphy for his support, as well as DESY for extending its hospitality to them. We are greatly indebted to the DESY Rechenzentrum, the Hallendienst and the synchrotron staff for their excellent cooperation and support. We thank Mr. K.H. Höhne and Mr. J.H. Weber for their assistance during the experiment. We also thank Dr. A. Ladage for the calibration of the beam, Dr. G. Schultze and Mr. F. Selonke for the construction and the test of the Čerenkov counter, and Miss H. Freier, Mr. J. Palm, Mr. R. Globisch and our scanning girls for their continued help. One of us (J.H.S.) received a Volkswagen foundation fellowship which made possible his stay at DESY.

Literature

- (1) C.W. Akerlof et al.,
Phys. Rev. Lett. 16, 147 (1966)
- (2) R. Kikuchi et al.,
Nuov. Cim. 43, 1178 (1966)
- (3) H. Blechschmidt et al.,
Proc. Int. Symp. on Electron and Photon Interactions,
p. 173, Hamburg 1965.
- (4) S. Berman,
Phys. Rev. 135, 1249 (1964)
- (5) M. Gourdin,
Nuov. Cim. 37, 209 (1965).
- (6) J.T. Beale, S.D. Ecklund, R.L. Walker,
CAL Inst. of Technology, Report CALT-68-108 (Nov. 1966).
- (7) G. Buschhorn et al.,
Phys. Rev. Lett. 17, 1027 (1966) and
Phys. Rev. Lett. 18, 572 (1967).

Figure Captions

Fig. 1 Experimental setup.

Figs.2a-c Spectrum of m_X for the reaction $e + p \rightarrow e' + \pi^\pm + X$ for 3 intervals of the energy of the virtual photon

- a) $0.7 \leq q_0 < 1.1$ GeV
- b) $1.1 \leq q_0 < 2.0$ GeV
- c) $2.0 \leq q_0 \leq 3.0$ GeV.

Figs.3a-c Number of events N as a function of q^2 weighted with the acceptance Acc for the reaction $e + p \rightarrow e' + \pi^\pm + n$ in 3 intervals of the energy of the virtual photon

- a) $0.7 \leq q_0 < 1.1$ GeV
- b) $1.1 \leq q_0 < 2.0$ GeV
- c) $2.0 \leq q_0 \leq 3.0$ GeV.

Figs.4a-c Differential cross section $\frac{d\sigma}{dt}$ for electroproduction as a function of the four momentum transfer t to the recoil nucleon for the reaction $e + p \rightarrow e' + \pi^\pm + n$ integrated over the accepted region of q^2 and averaged over the following intervals of the energy of the virtual photon

- a) $0.7 \leq q_0 < 1.1$ GeV
- b) $1.1 \leq q_0 < 2.0$ GeV
- c) $2.0 \leq q_0 \leq 3.0$ GeV.

Computed values for the cross section based on photo-production values are also shown.

Figs.5a-c Distribution of the azimuthal angle ϕ between the plane defined by the virtual photon and the pion and the plane defined by the incoming and outgoing electron weighted with the acceptance Acc' for the reaction $e + p \rightarrow e + \pi^\pm + n$ in 3 intervals of the energy of the virtual photon

- a) $0.7 \leq q_0 < 1.1$ GeV
- b) $1.1 \leq q_0 < 2.0$ GeV
- c) $2.0 \leq q_0 \leq 3.0$ GeV.

Acc' is calculated by integration over the accepted region of the azimuthal angle of the electron.

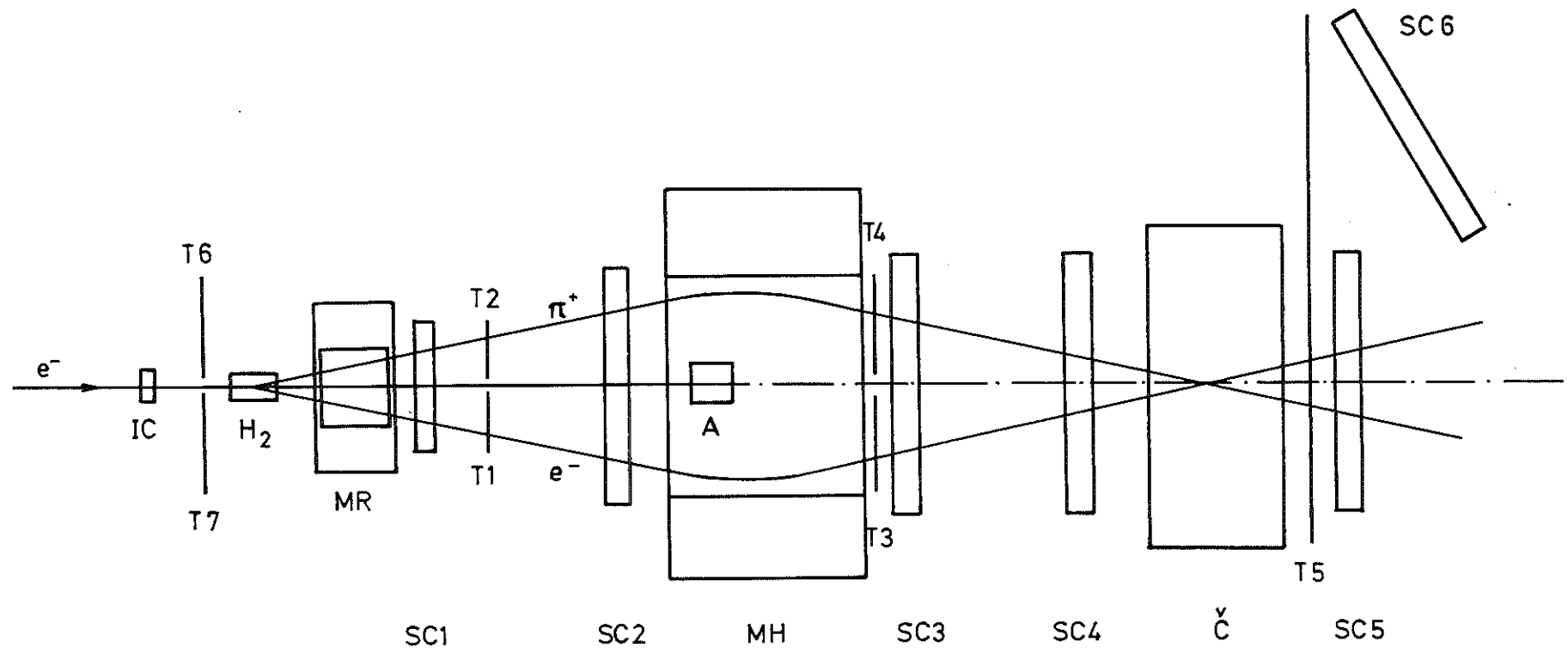
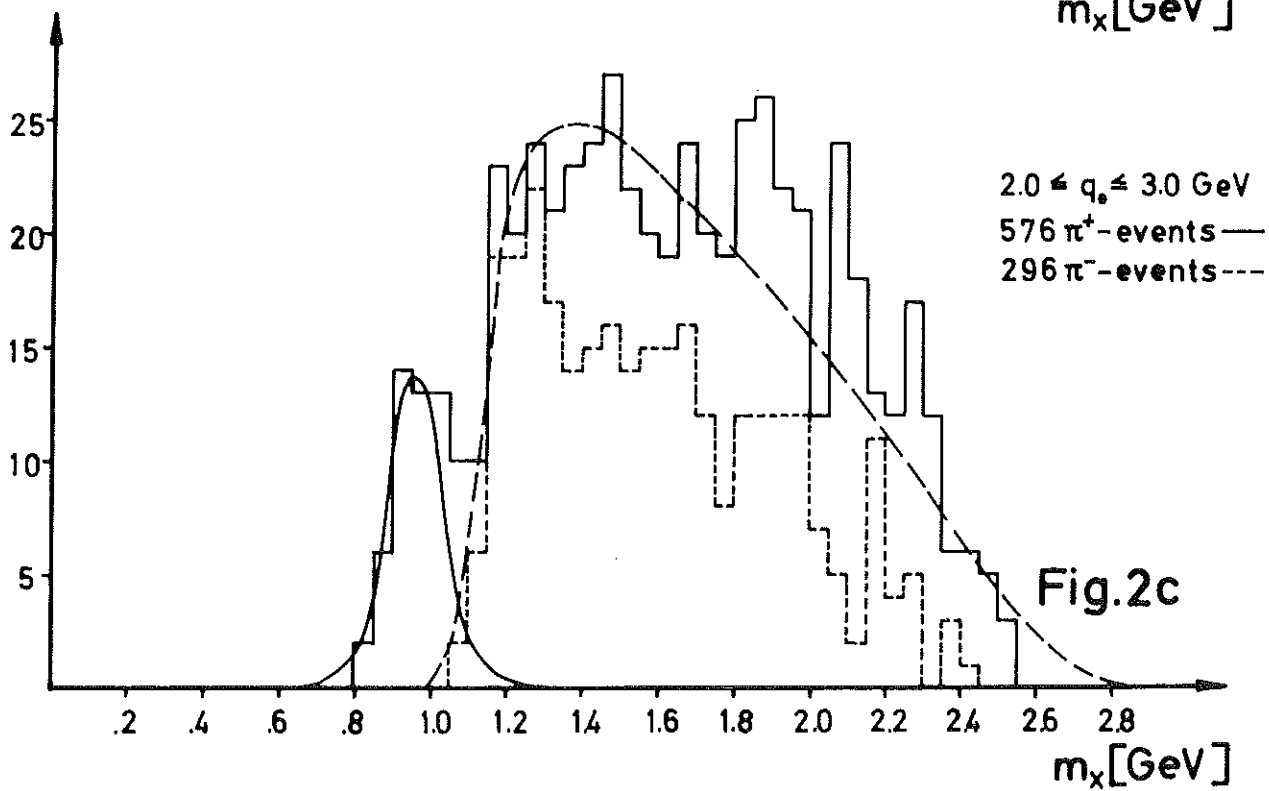
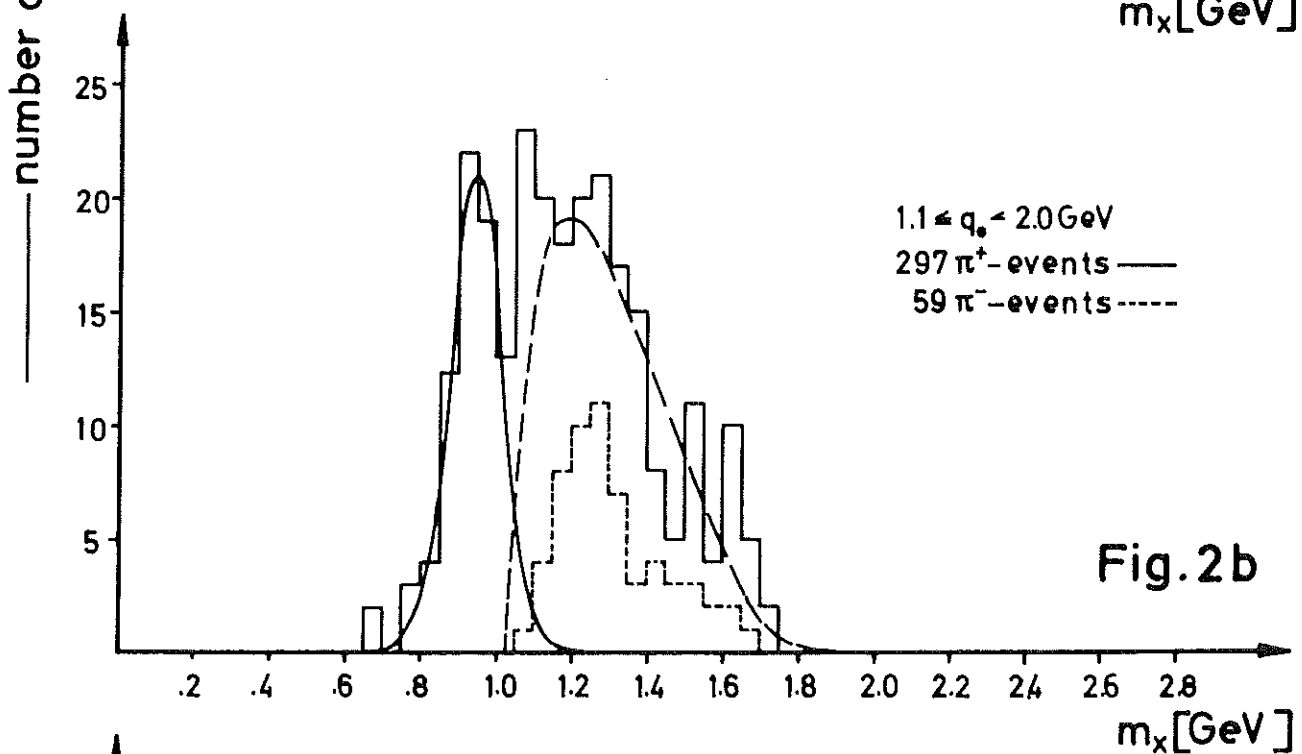
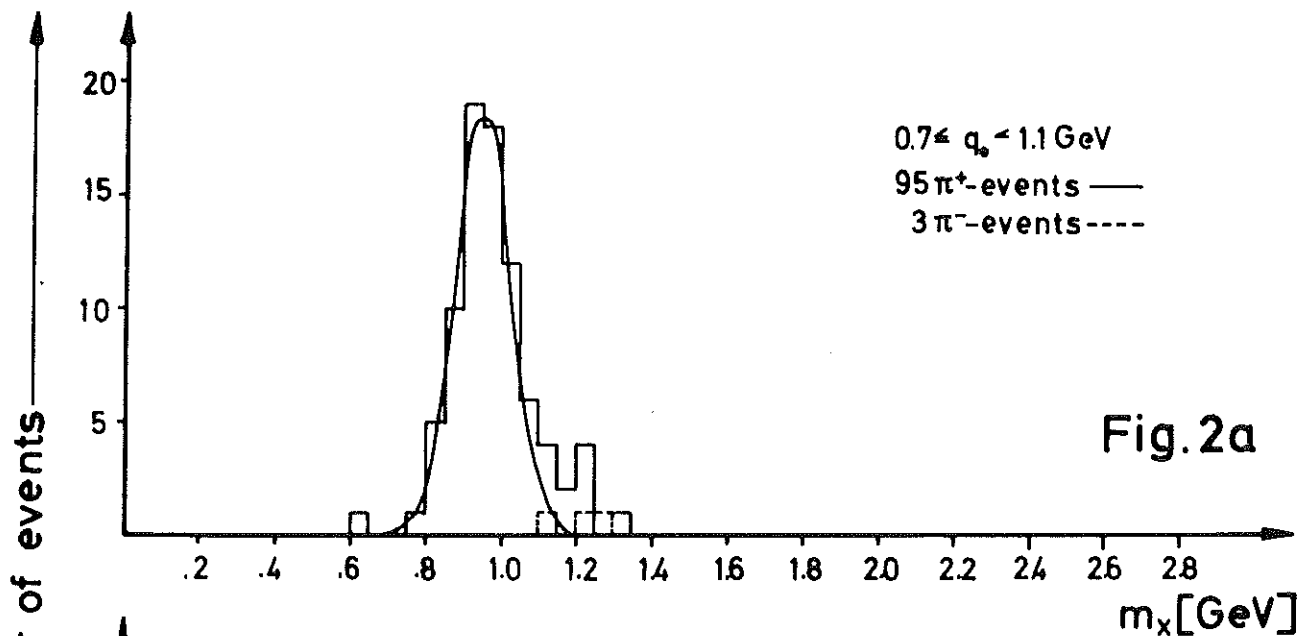


Fig.1



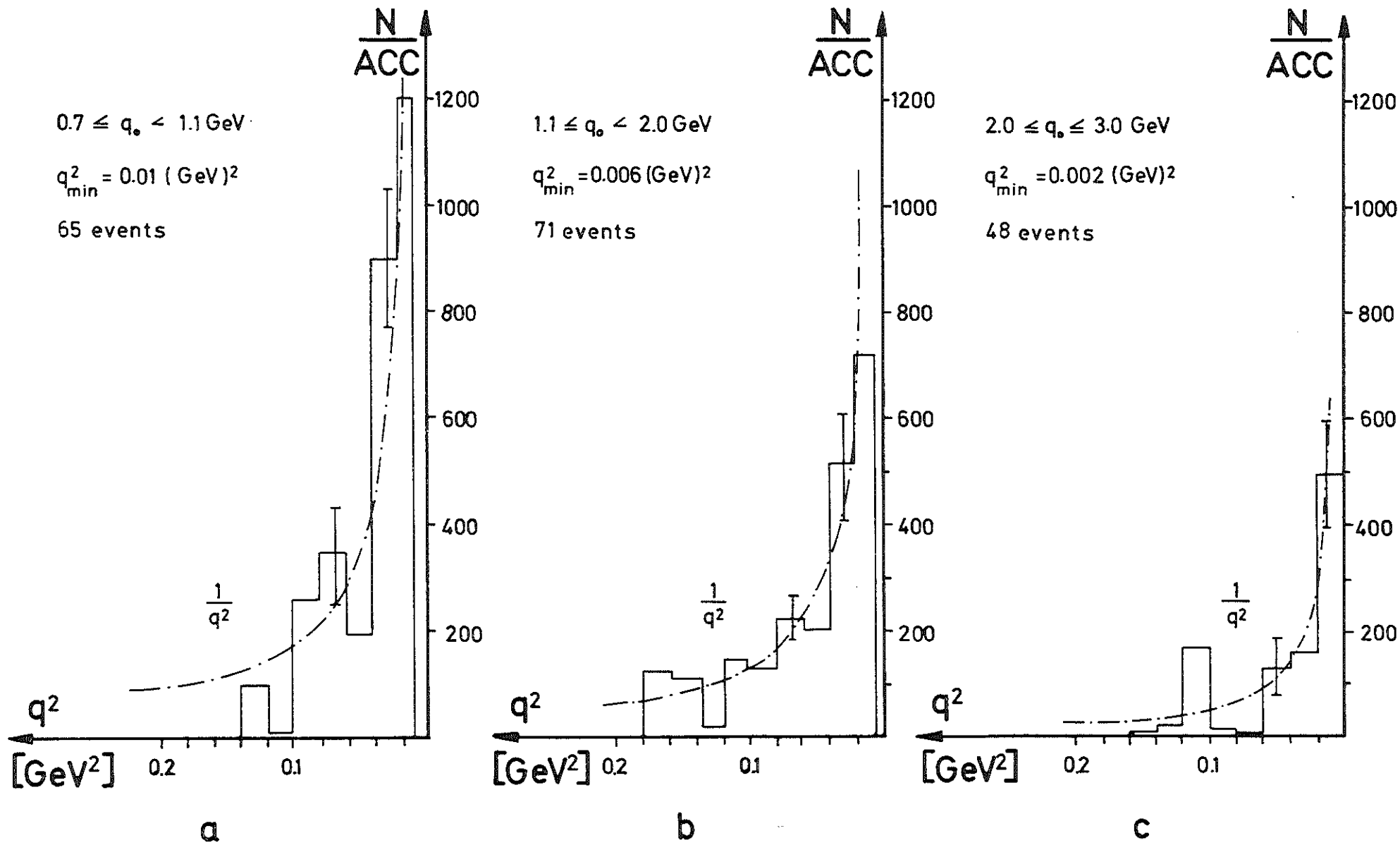


Fig. 3

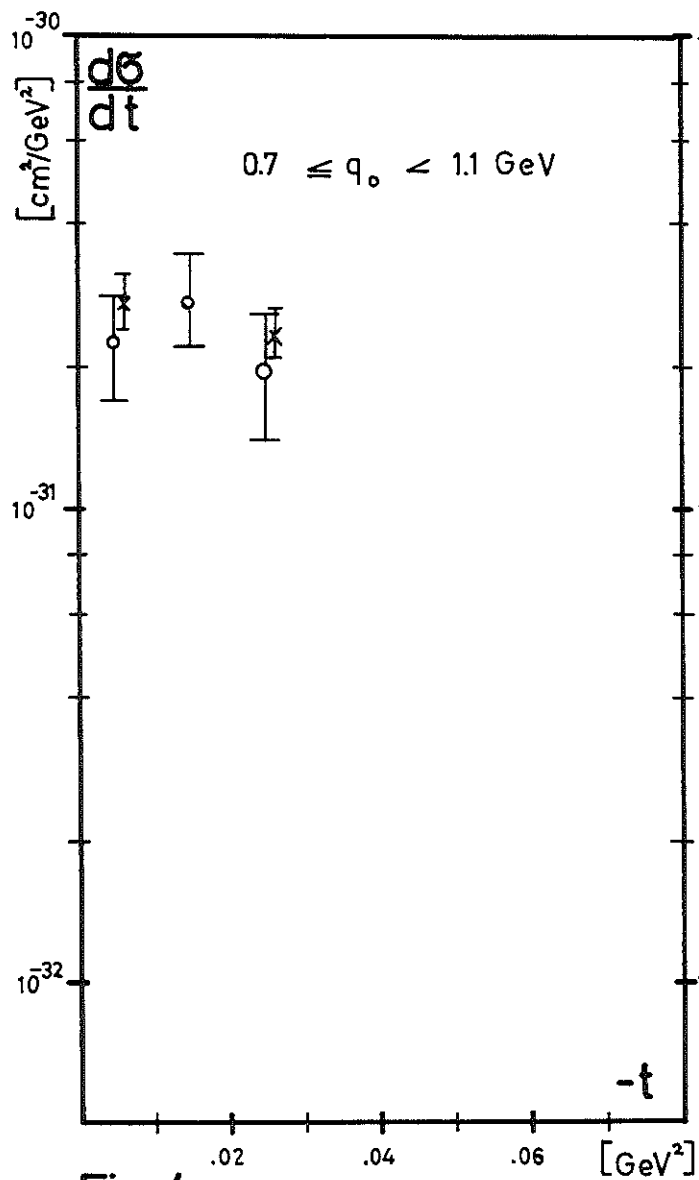


Fig.4a

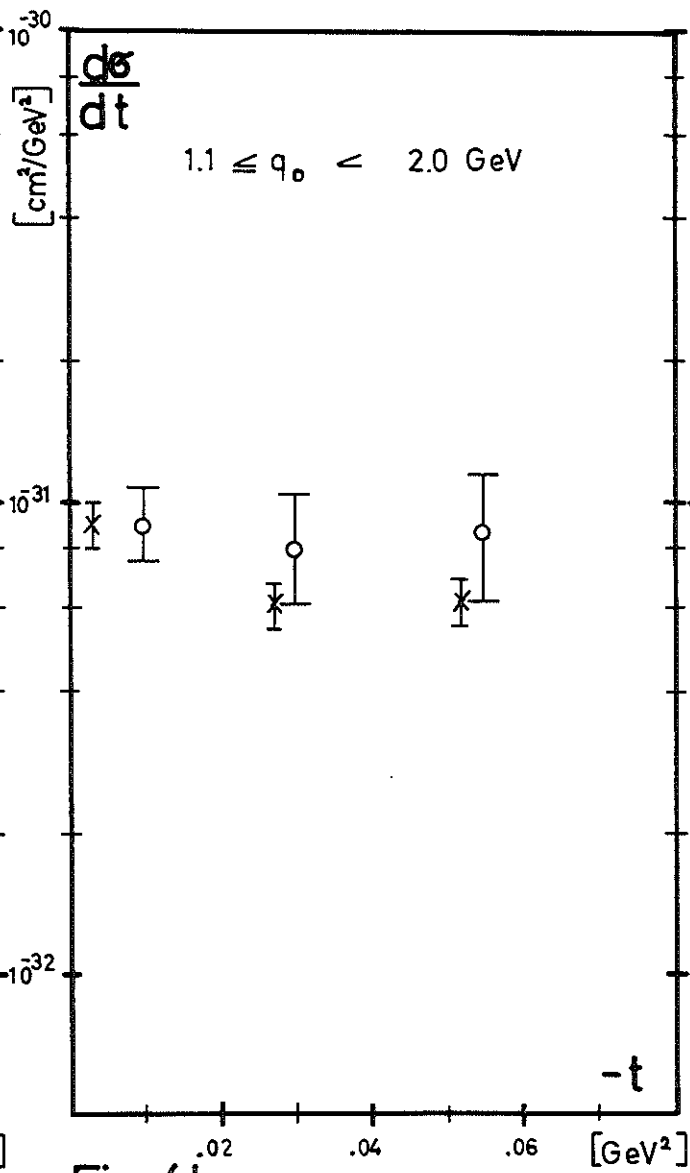


Fig.4b

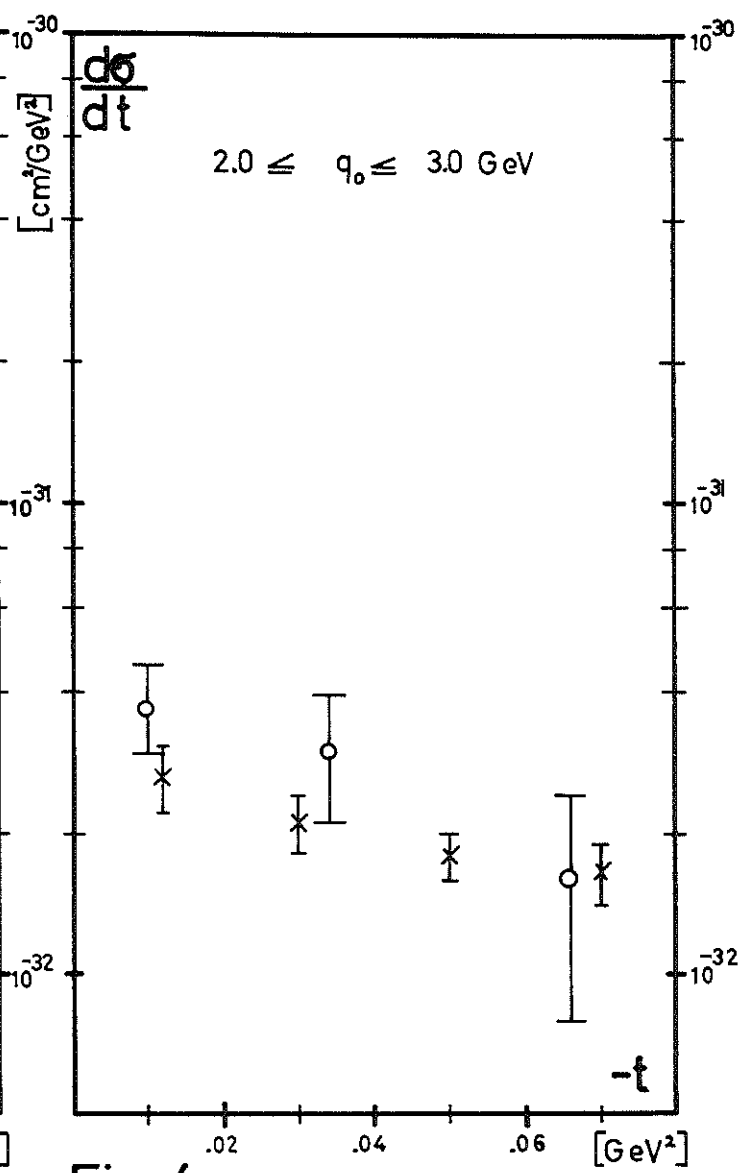




Fig.4c


 this experiment

 computed values from photoproduction
 (ref. 4,5)

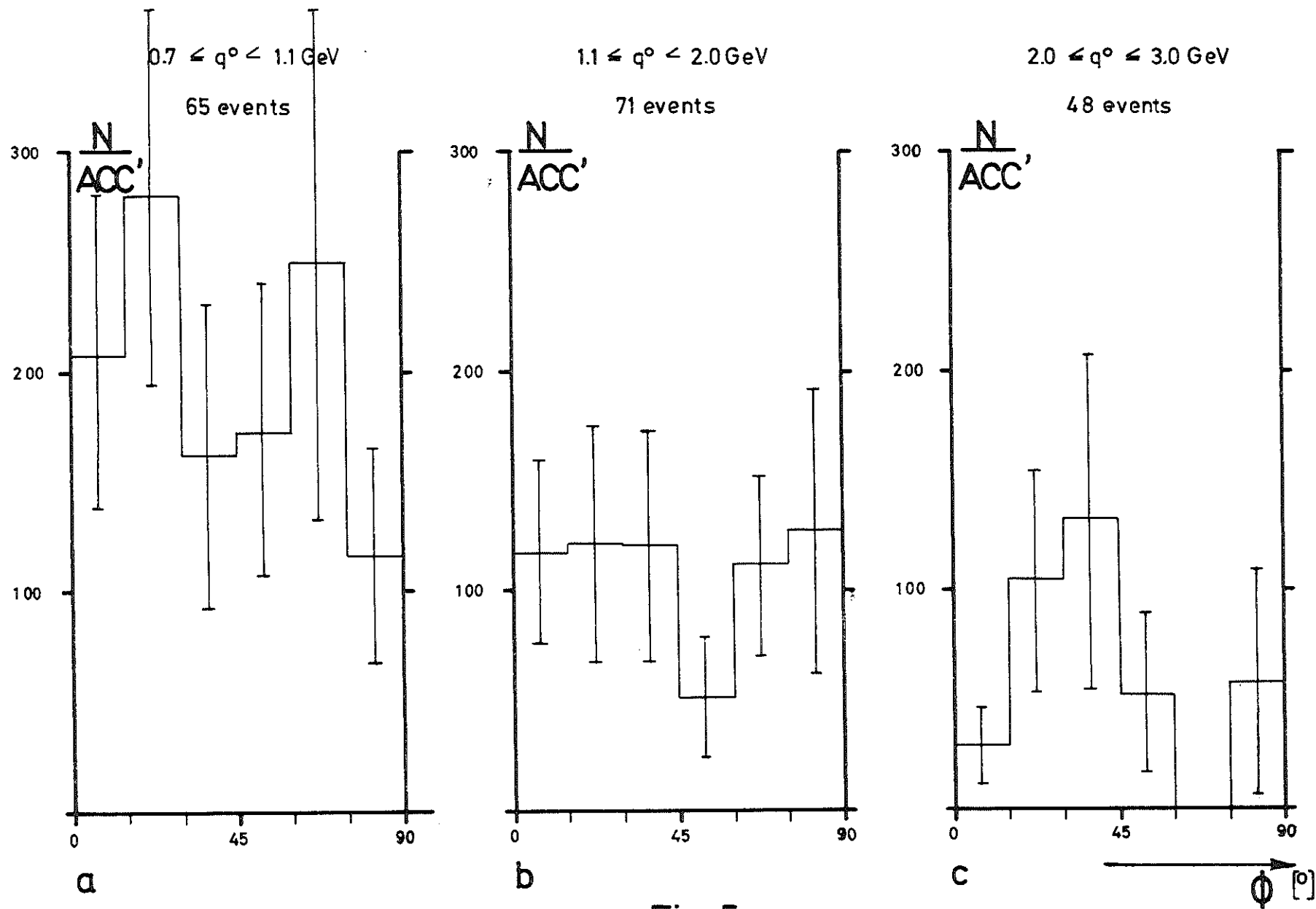


Fig. 5

